FIGURES

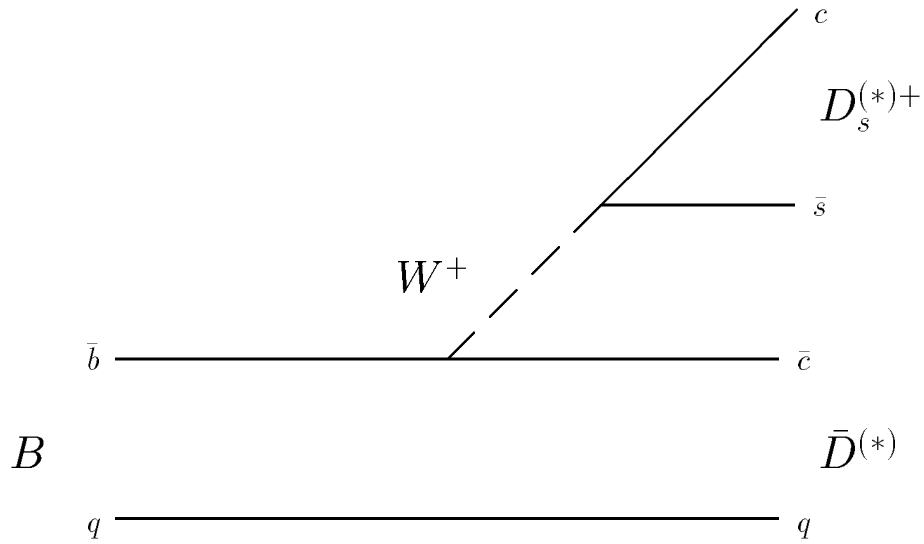

FIG. 1. The simple spectator diagram for hadronic B meson decay

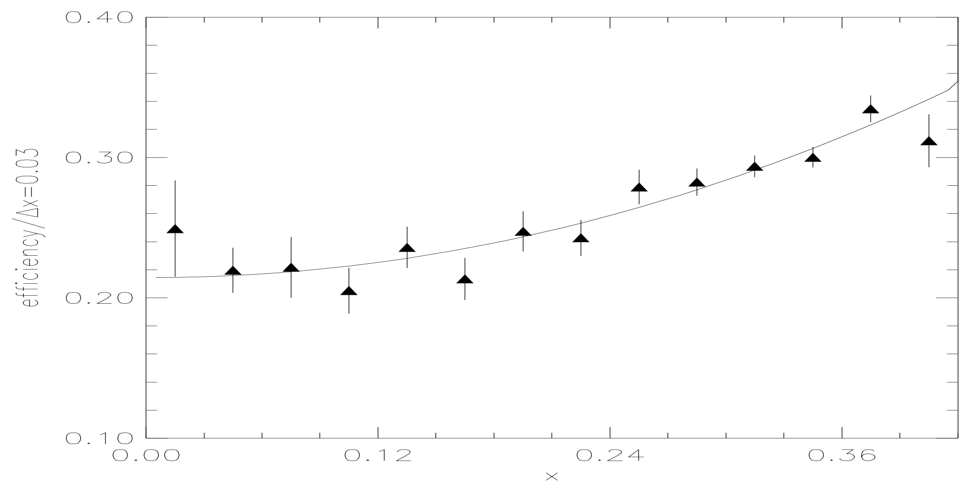

FIG. 2. The efficiency for reconstructing $D_s^+ \to \varphi\pi^+, \varphi \to K^+K^-$ as a function of scaled D_s^+ momentum for the cuts described in the text. The curve is the result of fitting a 2^{nd} order polynomial to the data points.

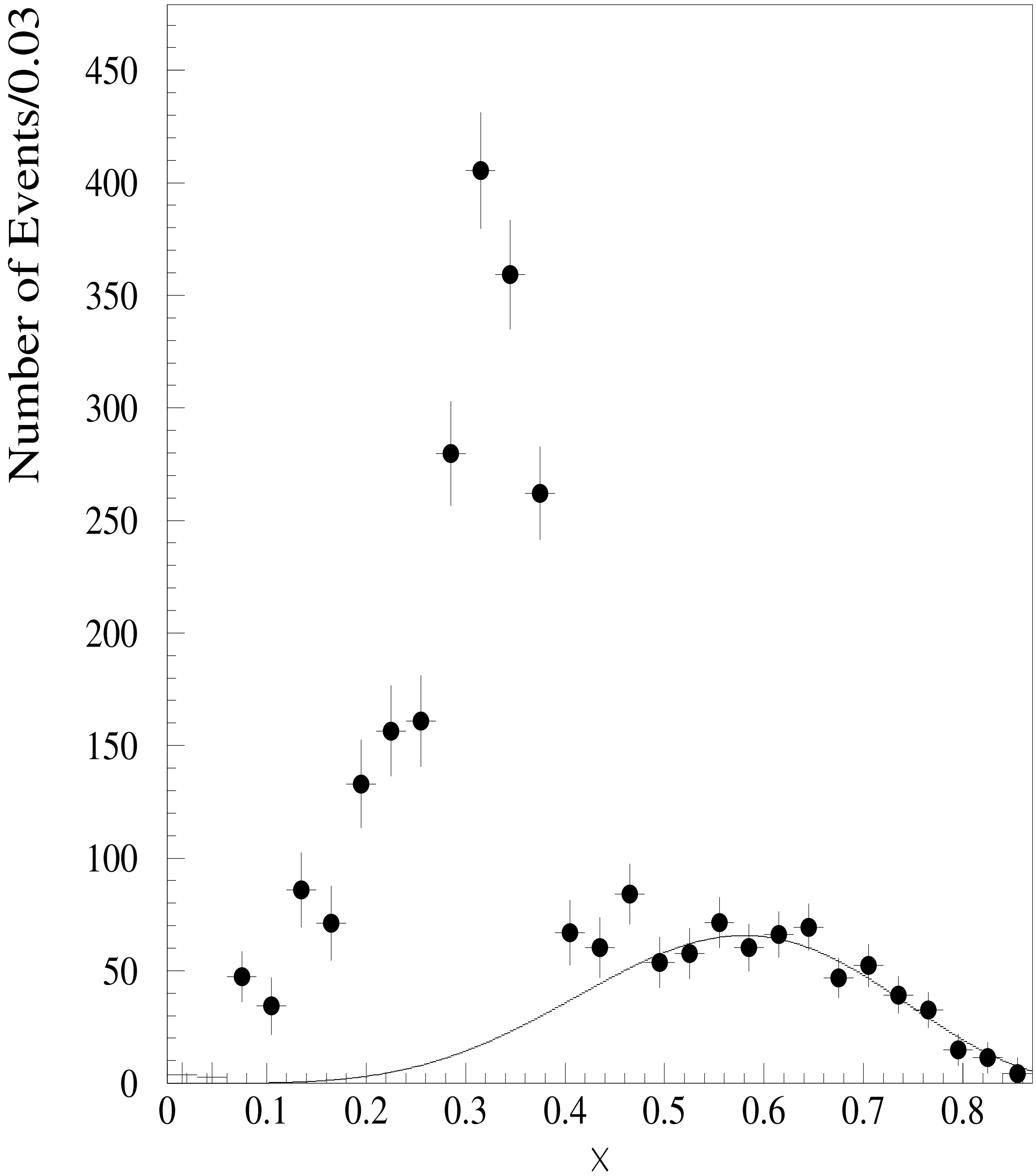

FIG. 3. The yield of D_s^+ mesons as a function of x before continuum subtraction and efficiency correction. The function is the result of the fit to the continuum D_s^+ momentum spectrum as described in the text. It is this function which is used to perform the continuum subtraction.

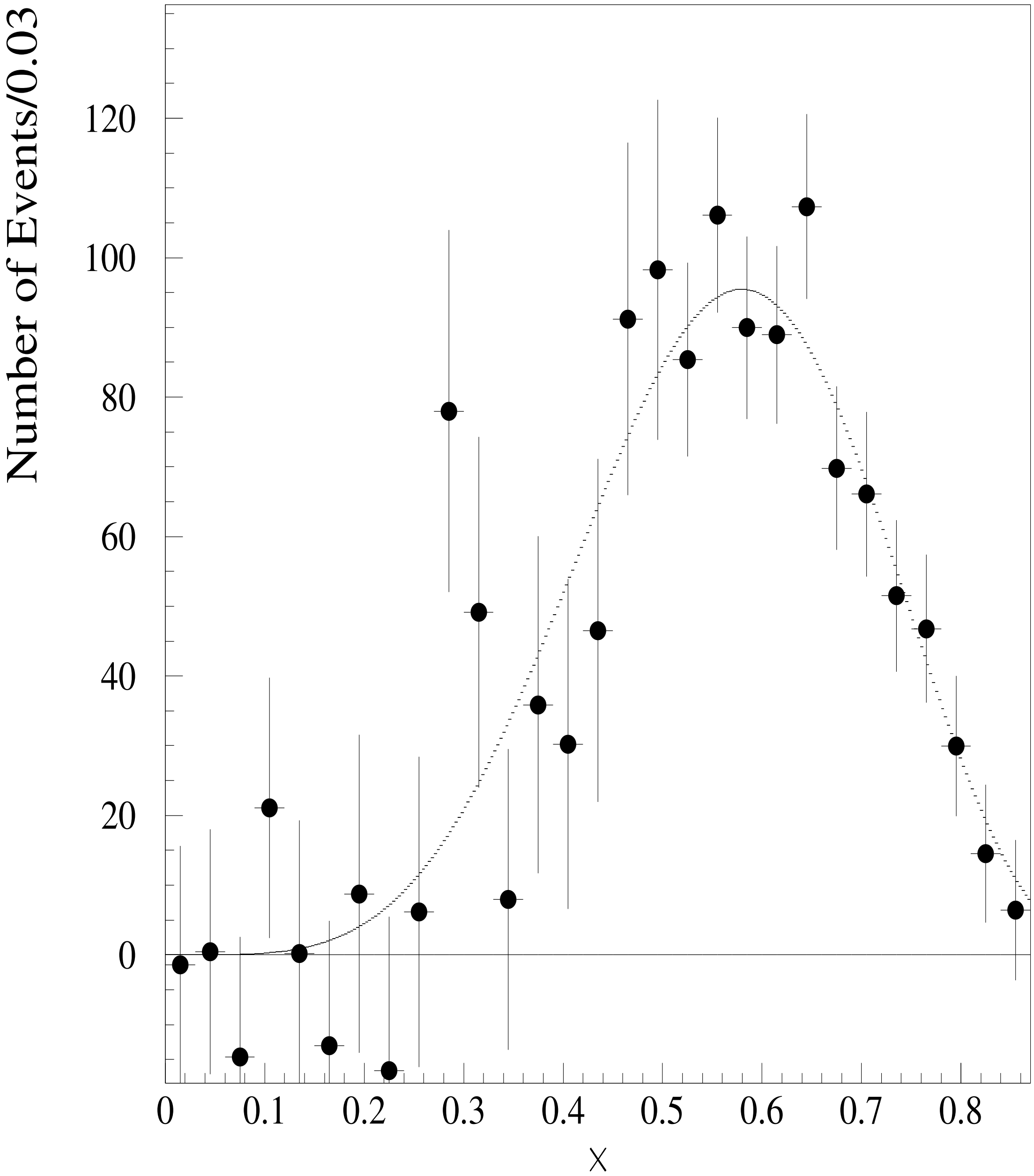

FIG. 4. The yield of continuum produced D_s^+ mesons as a function of x and the fit to the spectrum.

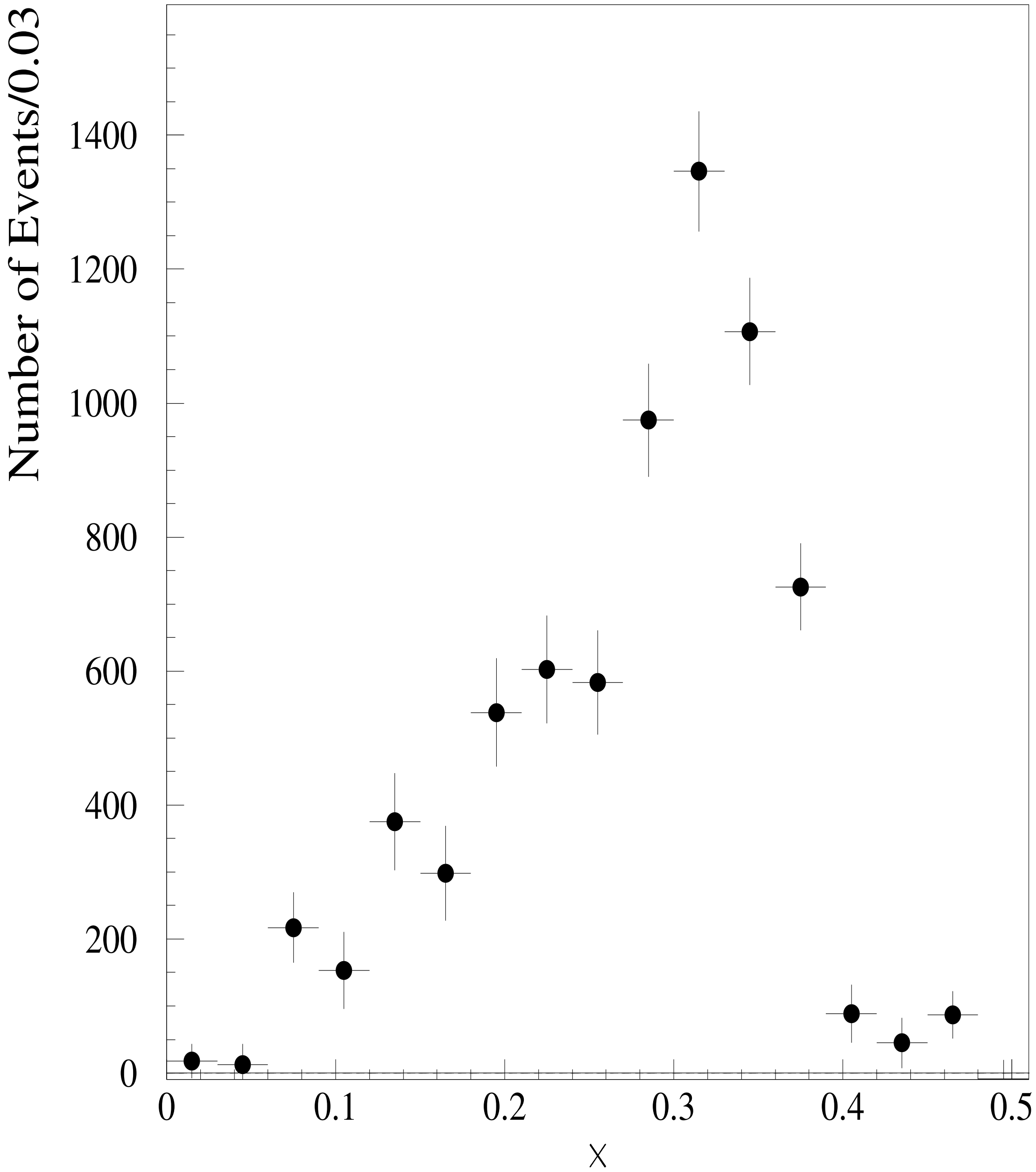

FIG. 5. The continuum-subtracted, efficiency-corrected yield of D_s^+ mesons as a function of x.

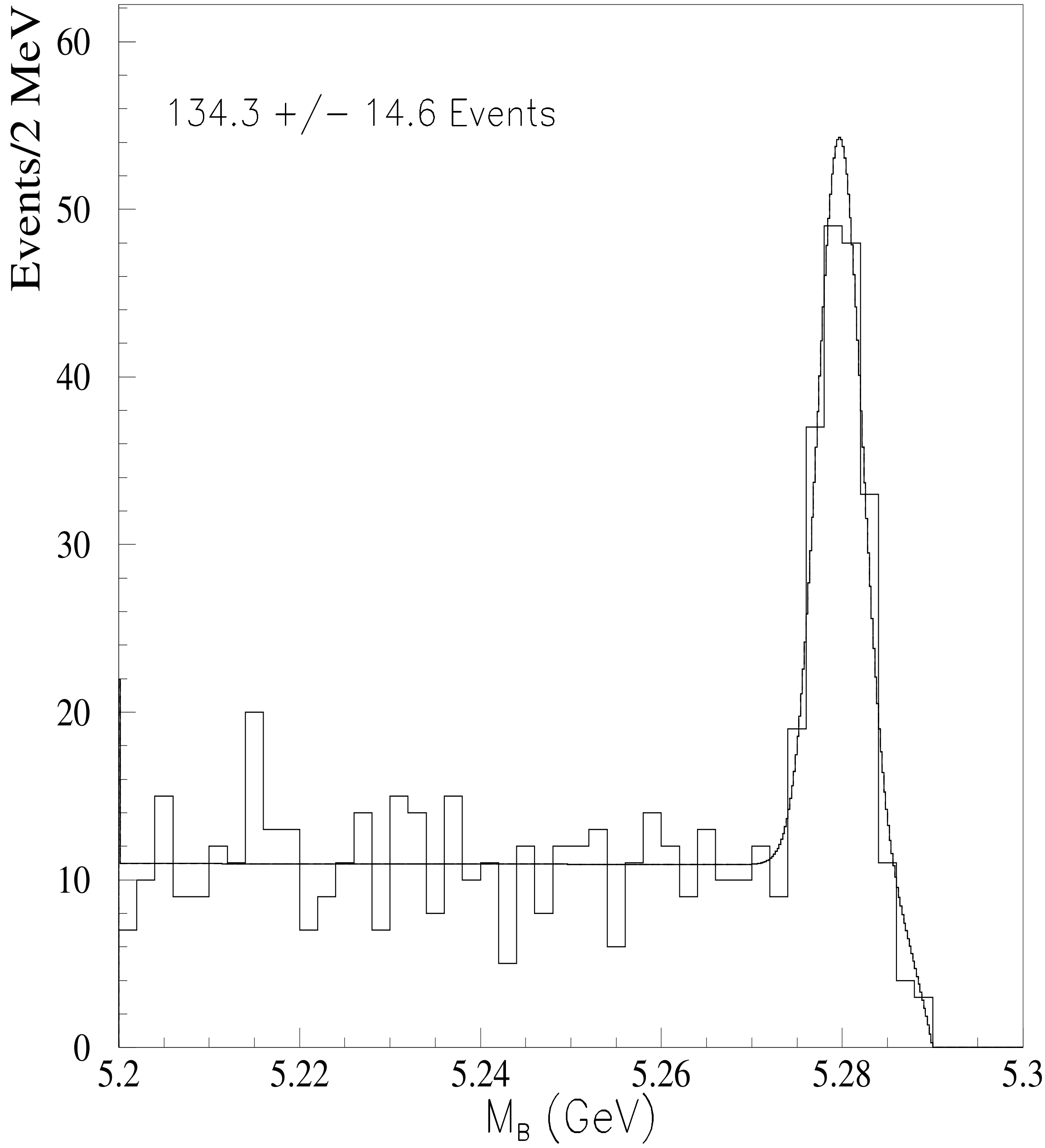

FIG. 6. The beam-constrained mass for the sum of the eight $B \to D_s^{(*)+} D^{(*)}$ modes.

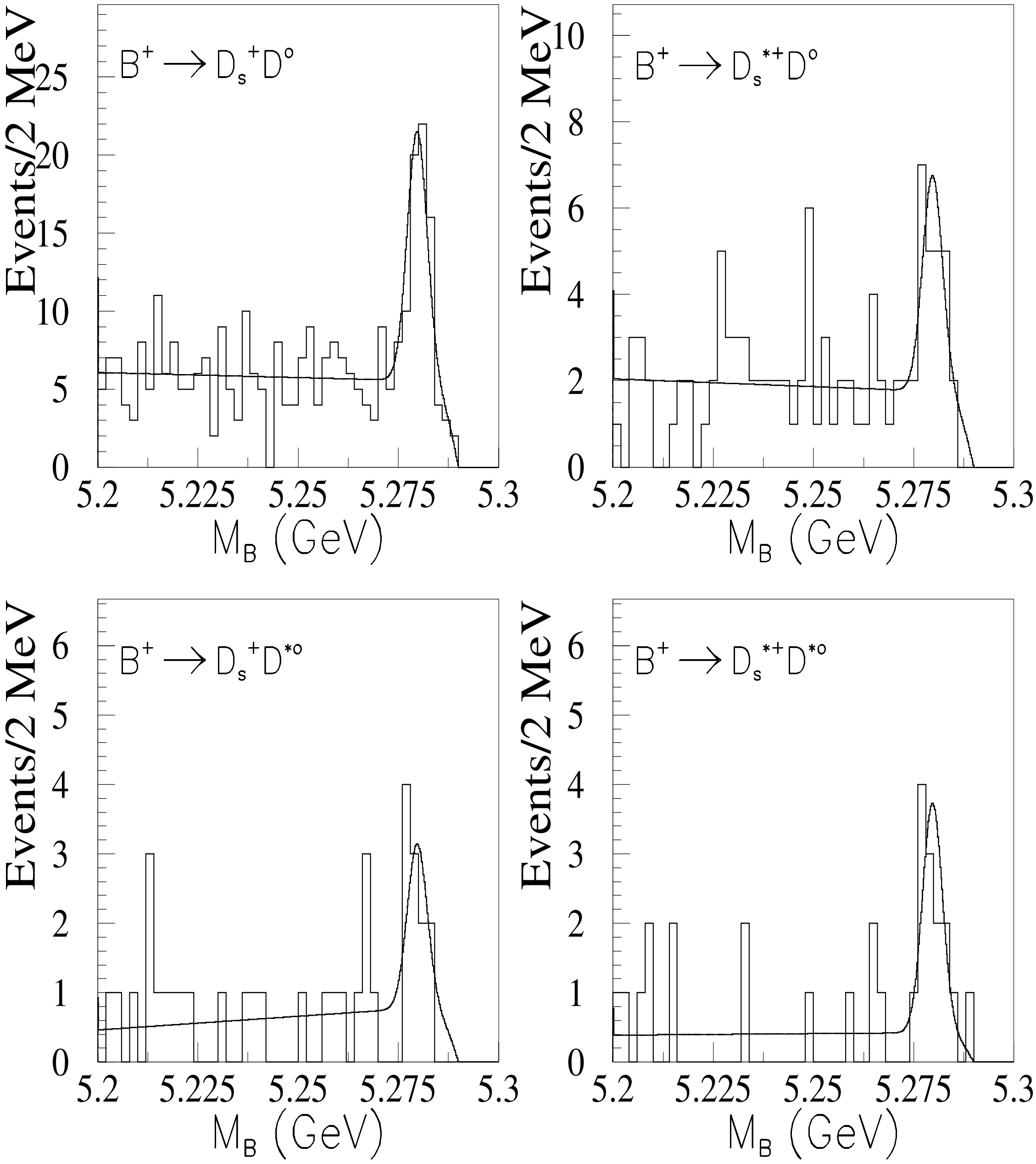

FIG. 7. The beam-constrained mass plots for B^+ decay modes.

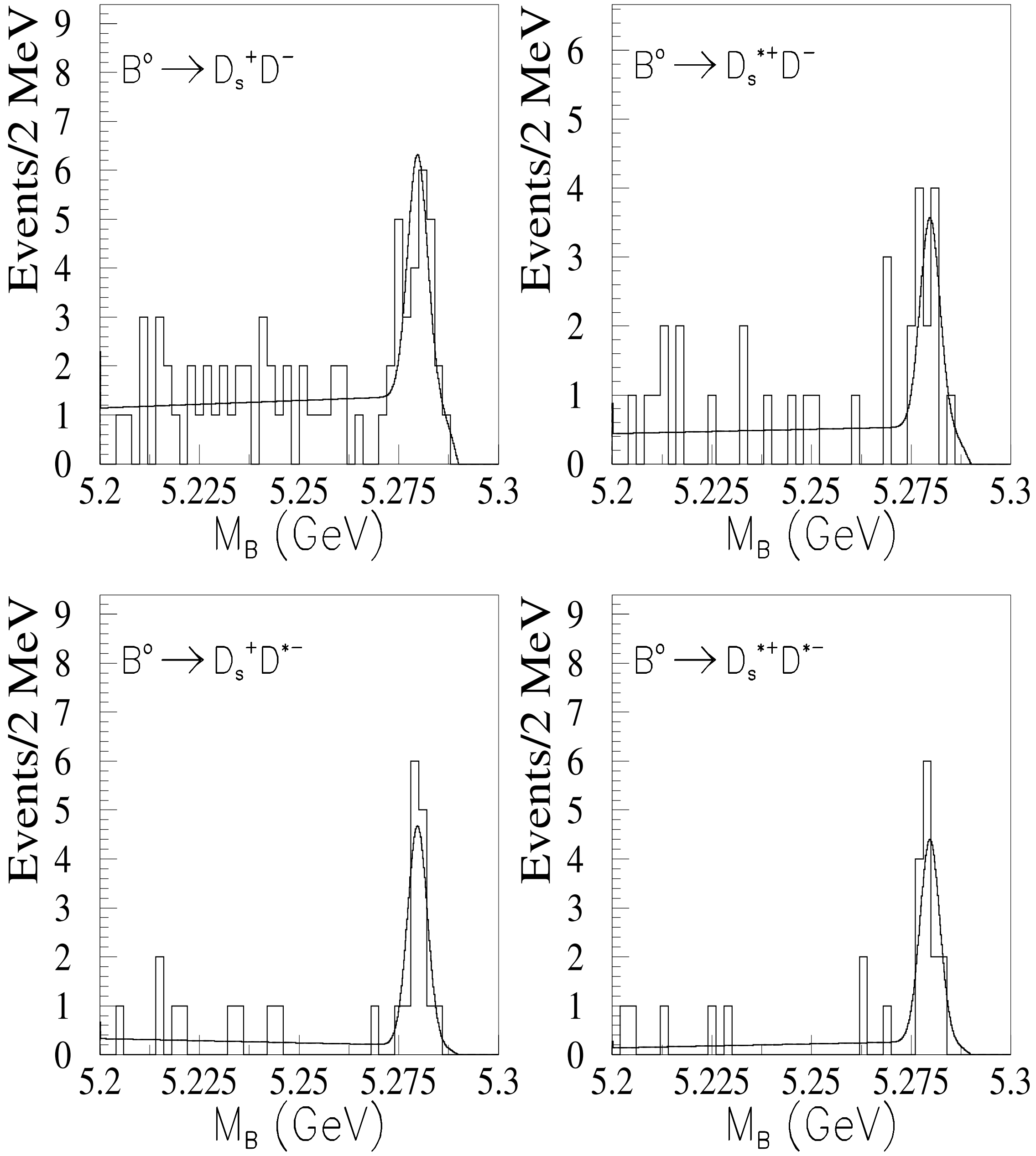

FIG. 8. The beam-constrained mass plots for B^o decay modes.

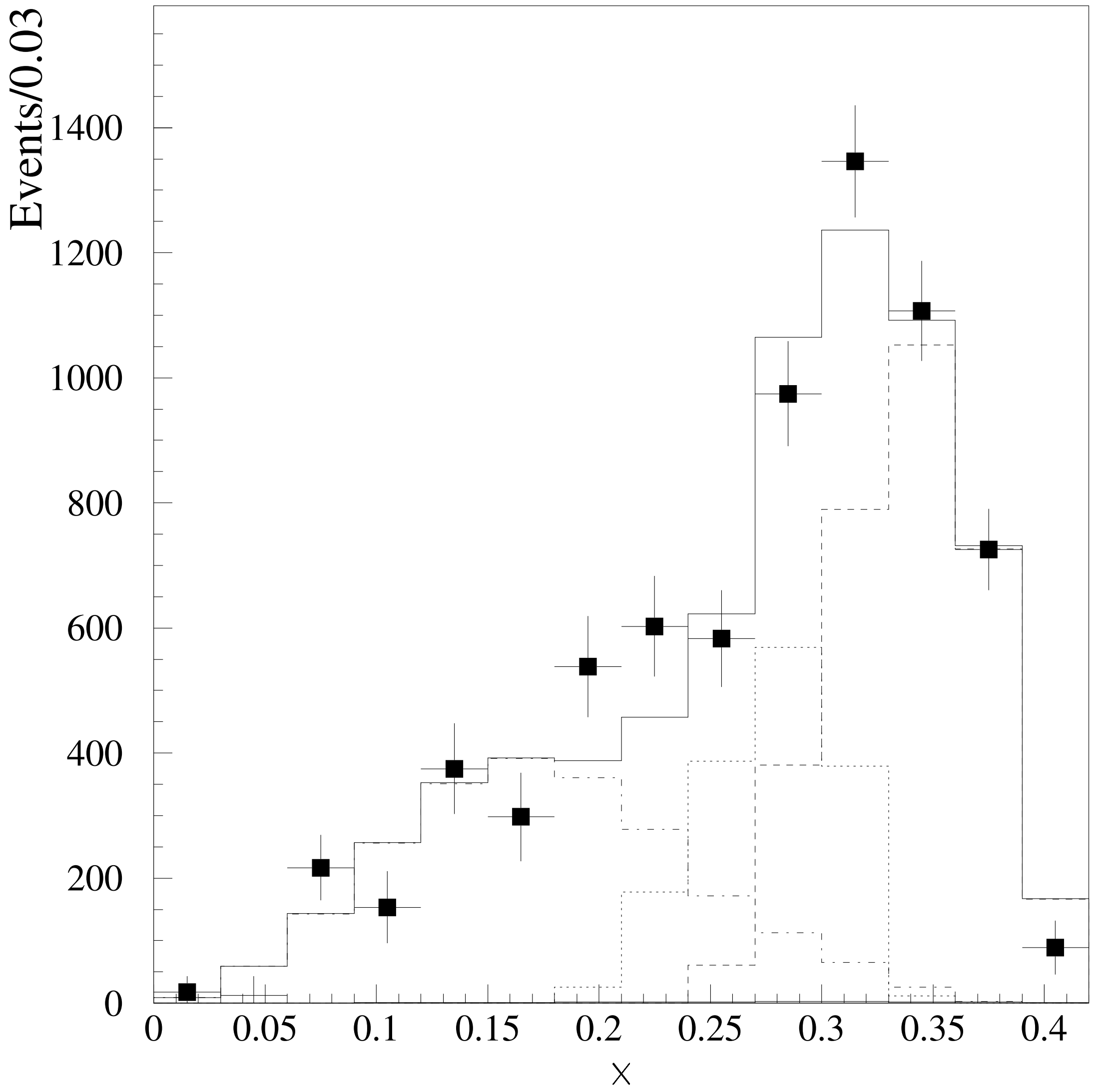

FIG. 9. An example fit to the D_s^+ momentum spectrum. The data points are the same as in Figure 4. The solid histogram is the result of the fit where the ratio of two-body widths has been fixed to the predictions of Neubert *et al.* as given in Table VII. Also shown are the individual components of the fitting function: the contribution from $B \to D_s^{(*)+}\bar{D}^{(*)}$ (dashed), $B \to D_s^{(*)+}\bar{D}^{**}$ (dotted), and $B \to D_s^{(*)+}\bar{D}^{(*)}\pi^{(*)}$ (dot-dash). The spectrum from lower-vertex decays was included in the fit but was found to be negligible.